CASE REPORT

Gliosarcoma after diagnosis of fibrillary astrocytoma

Tatsuya Kobayashi [a,b], Keiichi Sakai .[a,*], Tsuyoshi Tada [a], Yasuyuki Sekiguchi[a],

Yosuke Hara[a], Kunihiko Kodama [a], Tetsuya Goto[a], Yuichiro Tanaka [a], Kenji

Sano [c], Jun Nakayama [b], Kazuhiro Hongo[a]

[a] Department of Neurosurgery, Shinshu University School of Medicine, 3-1-1

Asahi, Matsumoto 390-8621, Japan

[b] Department of Pathology, Shinshu University School of Medicine,

Matsumoto, Japan

[c] Department of Laboratory Medicine, Shinshu University School of Medicine,

Matsumoto, Japan

*Corresponding author: Tel: +81 263 37 2690; fax: +81 263 37 0480

E-mail: skeiichi@ shinshu-u.ac.jp (K. Sakai).

Abstract

We report a 67-year-old woman was diagnosed with gliosarcoma at the second operation after being diagnosed with fibrillary astrocytoma at the primary operation. The patient underwent a CT-guided stereotactic biopsy. Histological examination showed fibrillary astrocytoma (World Health Organization [WHO] grade II). Loss of heterozygosity (LOH) on 1p, 10q, and 19q was not detected. She received chemotherapy, but no radiotherapy. Five months after the biopsy, MRI revealed rapid tumor growth. Tissue obtained from partial removal of the tumor revealed gliosarcoma (WHO grade IV), and LOH on 10q and 19q was detected. The history, histopathology, and genetic alterations of this patient are discussed.

1. **Introduction**

Gliosarcoma is a rare malignant neoplasm of the central nervous system that accounts for 2% to 8% of all patients with glioblastoma (1, 2). Gliosarcoma is defined as a glioblastoma variant with a biphasic tissue pattern of glial and mesenchymal differentiation, with significant clinical and genetic similarities (1, 3). The mechanism of pathogenesis in gliosarcoma is unclear. Most gliosarcomas are *de novo* at the time of the first resection for brain tumor, whereas others are diagnosed at the subsequent surgery for previously resected and irradiated glioblastoma (4, 5, 6). The former is termed primary gliosarcoma, and the latter is termed secondary gliosarcoma. However, malignant transformation from diffuse astrocytoma to gliosarcoma has not been previously described. We report a patient with gliosarcoma diagnosed at the second operation after diagnosis of fibrillary astrocytoma at the primary surgery.

2. **Case report**

2.1. History

A 67-year-old woman reported having dizzy episodes. A CT scan showed a high-density mass in her right hemisphere. Neurological examination revealed no apparent deficits. An MRI demonstrated a mass in the right corona radiata (Fig. 1A, B). Magnetic resonance (MR) spectroscopy showed no elevation of

lactate levels (Fig. 1C). A CT-guided stereotactic biopsy was performed of the slightly enhanced lesion on the MRI with preoperative fusion of the CT scan and MRI. The histological diagnosis was fibrillary astrocytoma (World Health Organization [WHO] grade II). The patient received 50 mg of ranimustine with interferon-β. She received no radiotherapy. Five months after the biopsy, follow-up MRI revealed rapid tumor growth, with projection into the right lateral ventricle (Fig. 1D, E). MR spectroscopy showed an elevated lactate level and a decline of N-acetylaspartate (Fig. 1F). The neurological symptoms now included head heaviness and mild right hemiparesis. The patient underwent surgery to partially remove the tumor located in the right lateral ventricle using a transcortical–transventricular approach. The tumor was grayish and reddish, rubbery, firm tissue that was not removable using suction. The histological examination showed gliosarcoma (WHO grade IV). Three months later, the patient died due to tumor progression. No autopsy was performed.

2.2   Histology at the first operation

On hematoxylin and eosin (H&E) staining of the tumor, cellularity was moderately increased, and nuclear atypia was mild. Mitosis, necrosis, and microvascular proliferation were absent (Fig. 2A). The tumor contained Rosenthal fibers (Fig. 2B), typical in brain areas with prolonged proliferation of astrocytes. Immunohistochemical (IHC) staining demonstrated many

astrocytes, with most cells testing positive for vimentin (Fig. 2E) and glial fibrillary acidic protein (GFAP) (Fig. 2F). The MIB-1 labeling index (LI) was less than 1% (Fig. 2C), and p53 expression was 11% (Fig. 2D). Silver staining showed no positive areas (Fig. 2G).

2.3   Histology at the second operation

Histological examination demonstrated a biphasic differentiation pattern with gliomatous and sarcomatous areas (Fig. 2H). In some regions, the gliomatous and sarcomatous components existed in a mosaic pattern. The gliomatous portion showed the typical features of glioblastoma, such as nuclear atypia, mitosis, necrosis, and microvascular proliferation. The sarcomatous portion showed spindle cells with nuclear atypia. IHC for vimentin (Fig. 2K) and GFAP (Fig. 2L) stained the tumor cells of the glial component, whereas the sarcomatous component contained a reticulin network visible with silver staining (Fig. 2M). The MIB-1 LI was 16% (Fig. 2I), and p53 expression was 20% (Fig. 2J).

2.4   Analysis of loss of heterozygosity

DNA was extracted from a paraffin-embedded sample of tumor tissue and corresponding peripheral blood. To enrich the tumor cell population, tumor areas were selected from the H&E-stained slides and isolated by

microdissection. Both the gliomatous and sarcomatous components were dissected. Loss of heterozygosity (LOH) of 1p, 10q, and 19q was assessed by polymerase chain reaction (PCR)-based microsatellite analysis. The following microsatellite markers were used: D1S468 and D1S1172 on chromosome 1p; D10S520 and D10S521 on chromosome 10q; D19S408, D19S601, and D19S867 on chromosome 19q. LOH on 1p, 10q, and 19q was not detected at the first operation. LOH on 10q and 19q was detected at the second operation (Fig. 3).

3. **Discussion**

Gliosarcoma was first described by Stroebe et al. in 1895 (7) and gained general acceptance through the landmark papers of Feigen and Gross (8) and Rubinstein et al. (9). In the present patient, the tumor from the second operation displayed a biphasic differentiation pattern with glial and sarcomatous components. The sarcomatous area showed a reticulin network on silver staining. IHC for GFAP stained the tumor cells of the glial component, and silver staining was absent in glial areas. These features are diagnostic of gliosarcoma. However, the initial diagnosis of the tumor from the first operation was fibrillary astrocytoma. Astrocytomas frequently demonstrate considerable histopathological heterogeneity, with focal areas of more malignant features spread among regions with a more benign appearance (10,

11). Because of the heterogeneous organization of gliosarcoma tumors, the first biopsy may have been malignant glioma with sampling error. However, we performed the CT-guided stereotactic biopsy of the slightly enhanced lesion accurately with preoperative fusion of CT scans and MRI. Moreover, the tumor from the first operation showed Rosenthal fibers, which indicated that the tumor had grown slowly over a longer time. Follow-up MR spectroscopy indicated malignant change at the recurrence. In the present patient, the tumor appears to have transformed from fibrillary astrocytoma into gliosarcoma. To our knowledge, there have been no prior reports of such a rapid malignant transformation from diffuse astrocytoma to gliosarcoma.

  Glioblastomas develop *de novo* (primary glioblastomas) or through progression from low-grade or anaplastic astrocytomas (secondary glioblastoma). Recent studies have shown that these glioblastoma subtypes develop through different genetic pathways. Primary glioblastomas are characterized by epidermal growth factor receptor (*EGFR*) amplification/ overexpression, *p16* deletion, *PTEN* mutation, and LOH on entire chromosome 10, whereas secondary glioblastomas typically contain *p53* mutations and show LOH on chromosome 10q (12, 13, 14). Additionally, LOH on 19q is more frequent in secondary glioblastomas than in primary glioblastomas (15). Gliosarcomas have genetic aberrations, such as *p53* mutation, *PTEN* mutation, and *p16* deletion, similar to those of primary glioblastomas (3). Primary and

secondary glioblastomas are derived from differentiated astrocytes or precursor cells with different genetic pathways. Actor et al. reported that the genomic alterations in gliosarcomas are closely related to those found in primary glioblastomas (16). In the present patient, p53 expression of the first tumor was 11%, which is moderately high. Moreover, LOH on 10q and 19q was detected in the specimen from the second operation, but not from the first operation. These changes are more characteristic of secondary glioblastoma. There have been no reports of genetic analyses of secondary gliosarcoma. The history, histopathology, and genetic alterations of our patient indicate a unique occurrence of gliosarcoma. Reports of of gliosarcoma are few. Further studies including large numbers of patients are necessary to elucidate the mechanisms underlying gliosarcoma.

References

1. Galanis E, Buckner JC, Dinapoli RP, et al. Clinical outcome of gliosarcoma compared with glioblastoma multiforme: North Central Cancer Treatment Group results. *J Neurosurg* 1998;**89**:425-30.

2. Meis JM, Ho KL, Nelson JS. Gliosarcoma: a histologic and immunohistochemical reaffirmation. *Mod Pathol* 1990;**3**:19-24.

3. Reis RM, Konu-Leblebicioglu D, Lopes JM, Lopes JM, Kleihues P, Ohgaki

H. Genetic profile of gliosarcomas. *Am J Pathol* 2000;**156**:425-32.

4. Han SJ, Yang I, Tihan T, Chang SM, Parsa AT. Secondary gliosarcoma: a review of clinical features and pathological diagnosis. *J Neurosurg* 2010;**112**:26-32.

5. Han SJ, Yang I, Tihan T, Prados MD, Parsa AT. Primary gliosarcoma: key clinical and pathologic distinctions from glioblastoma with implications as a unique oncologic entity. *J Neurooncol* 2010;**96**:313-20.

6. Perry JR, Ang LC, Bilbao JM, Muller PJ. Clinicopathologic features of primary and postirradiation cerebral gliosarcoma. *Cancer* 1995;**75**:2910-8.

7. Stroebe H. Uber Entstehung und Bau der Hirngliome. *Beitr Pathol Anat* 1895;**18**:405-86.

8. Feigin IH, Gross SW. Sarcoma arising in glioblastoma of the brain. *Am J Pathol* 1955;**31**:633-53.

9. Rubinstein LJ. The development of contiguous sarcomatous and gliomatous tissue in intracranial tumours. *J Pathol Bacteriol* 1956;**71**:441-59.

10. DeAngelis LM. Brain tumors. *N Engl J Med* 2001;**344**:114-23.

11. Frappaz D, Chinot O, Bataillard A, et al. Summary version of the standards, options and recommendations for the management of adult patients with intracranial glioma (2002). *Br J Cancer* 2003;**89**:S73-S83.

12. Biernat W, Tohma Y, Yonekawa Y, Kleihues P, Ohgaki H. Alterations of cell cycle regulatory genes in primary (de novo) and secondary

glioblastomas. *Acta Neuropathol* 1997;**94**:303-9.

13. Tohma Y, Gratas C, Biernat W, et al. PTEN (MMAC1) mutations are frequent in primary glioblastomas (de novo) but not in secondary glioblastomas. *J Neuropathol Exp Neurol* 1998;**57**:684-9.

14. Watanabe K, Tachibana O, Sata K, Yonekawa Y, Kleihues P, Ohgaki H. Overexpression of the EGF receptor and p53 mutations are mutually exclusive in the evolution of primary and secondary glioblastomas. *Brain Pathol* 1996;**6**:217-24.

15. Nakamura M, Yang F, Fujisawa H, Yonekawa Y, Kleihues P, Ohgaki H. Loss of heterozygosity on chromosome 19 in secondary glioblastomas. *J Neuropathol Exp Neurol* 2000;**59**:539-43.

16. Actor B, Cobbers J.M.J. L, Buschges R, et al. Comprehensive analysis of genomic alterations in gliosarcoma and its two tissue components. *Genes, Chromosomes & Cancer* 2002;**34**:416-27.

Figure legends

Fig. 1. (A) Axial fluid-attenuated inversion recovery and (B) axial gadolinium (Gd)-enhanced T1-weighted MRI taken before the first operation showing a mass with slight enhancement in the right corona radiata. (C) Magnetic resonance (MR) spectroscopy showing no elevation of lactate (Lac). (D) Axial FLAIR and (E) axial Gd-enhanced T1-weighted MRI images taken before the second operation showing rapid growth of the tumor with a well-enhanced lesion. (F) MR spectroscopy shows an elevation of Lac levels and a decline of N-acetylaspartate (NAA).

Fig. 2. Photomicrographs of the tumor at the first operation (A–G) showing: (A) cellularity is moderately increased, and nuclear atypia is mild, and mitosis, necrosis and microvascular proliferation is absent, and (B) the presence of Rosenthal fibers (hematoxylin and eosin [H&E]). Immunohistochemistry (IHC) staining showing: (C) that MIB-1 labeling index (LI) is < 1% (Ki-67 IHC), (D) p53 expression is 11%, (E) most tumor cells are positive for vimentin, and (F) glial fibrillary acidic protein (GFAP), but (G) that no cells stained positive with silver staining. Photomicrographs at the second operation (H–M) showing: (H) a biphasic differentiation pattern (gliomatous, with nuclear atypia, mitosis, necrosis, and microvascular proliferation; and sarcomatous, with spindle cells with nuclear atypia) (H&E). Immunohistochemistry (IHC) for (I) Ki-67

showing the MIB-1 LI is 16% and (J) p53 expression is 20%. Some gliomatous

and sarcomatous parts are positive for (K) vimentin and (L) GFAP. (M) The

sarcomatous part contains a reticulin network on silver staining. All bars

represent 100 µm (A, C–M), except for (B), 50 µm.

Fig. 3. Loss of heterozygosity(LOH) analysis of DNA extracted from (B)

blood, (G) the gliomatous component, and (S) the sarcomatous component

showing that: (upper – from the first operation) LOH on 1p, 10q, and 19q is not

detected in the tumor; and (lower – from the second operation) LOH on 19q is

detected in the gliomatous component; LOH on 10q and 19q is also detected in
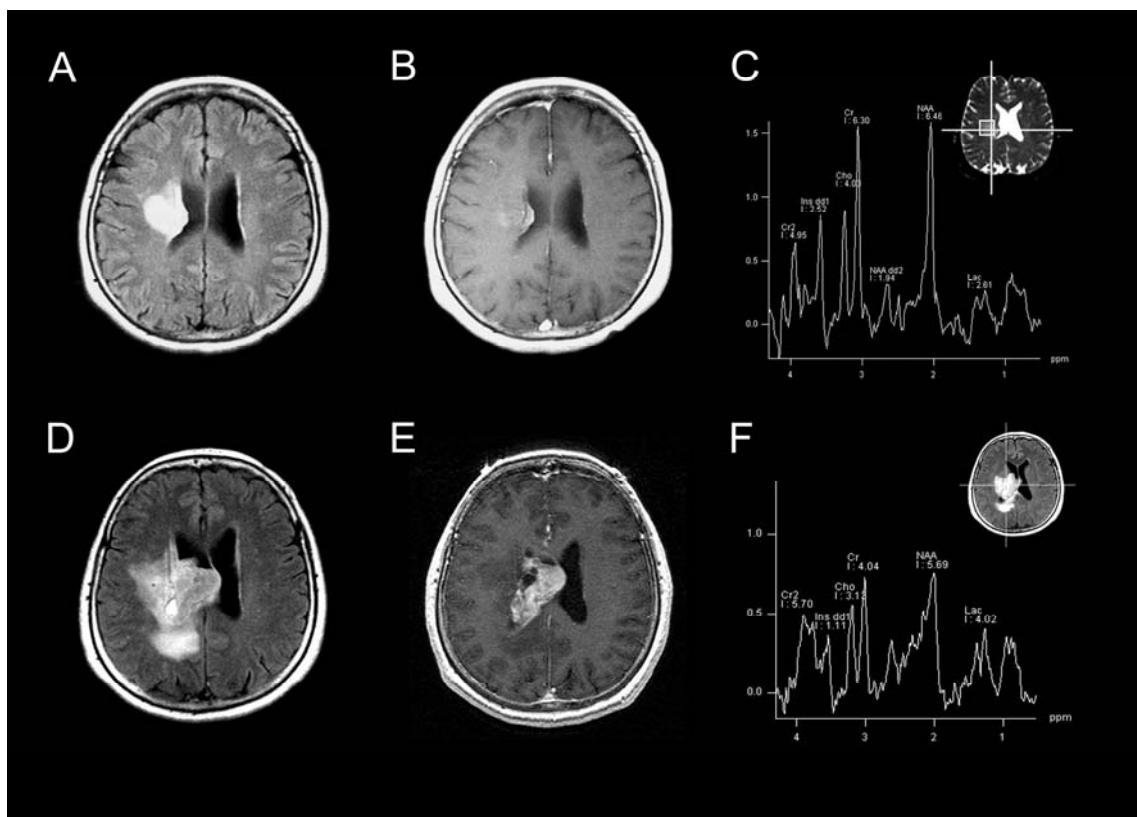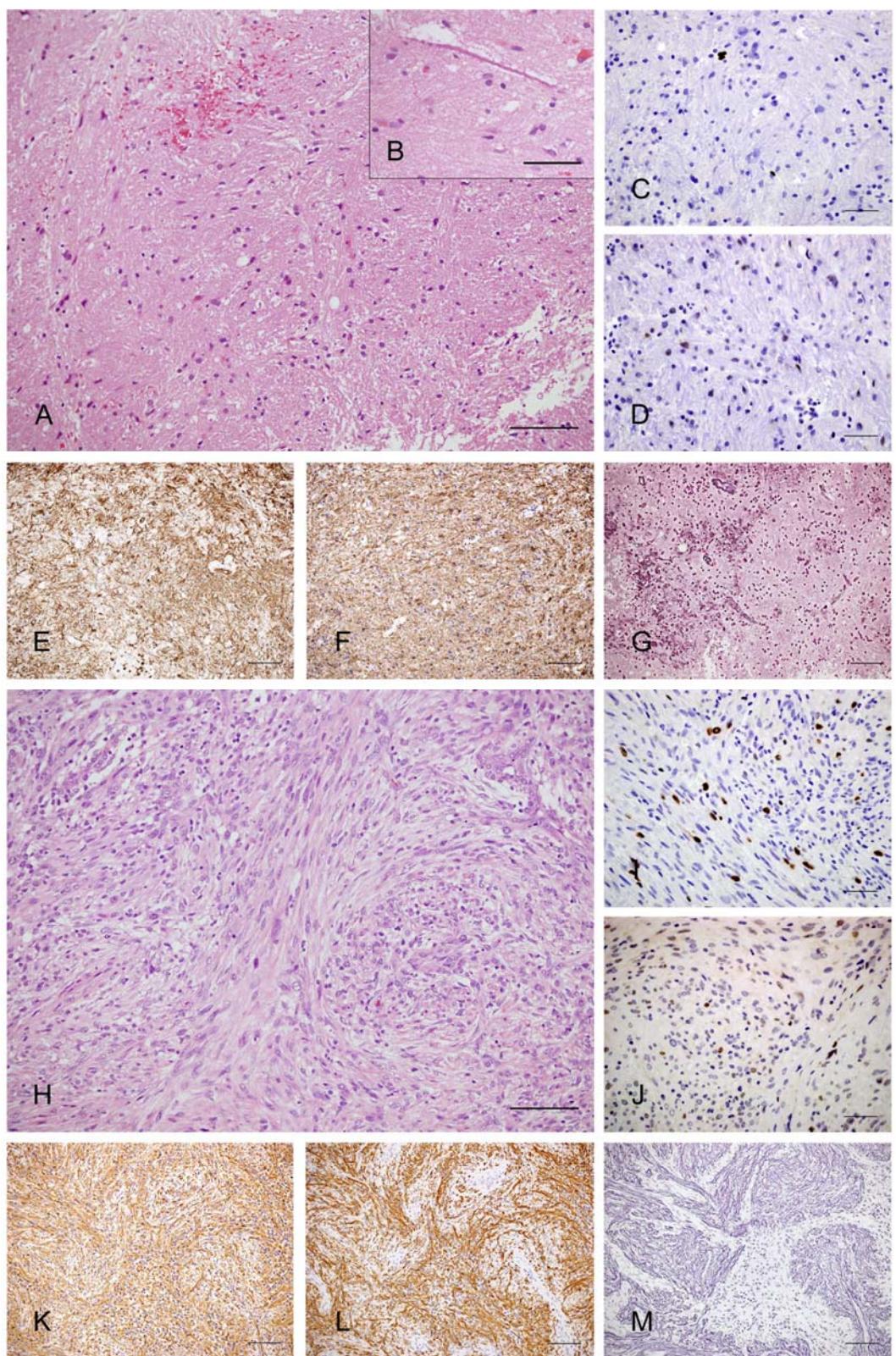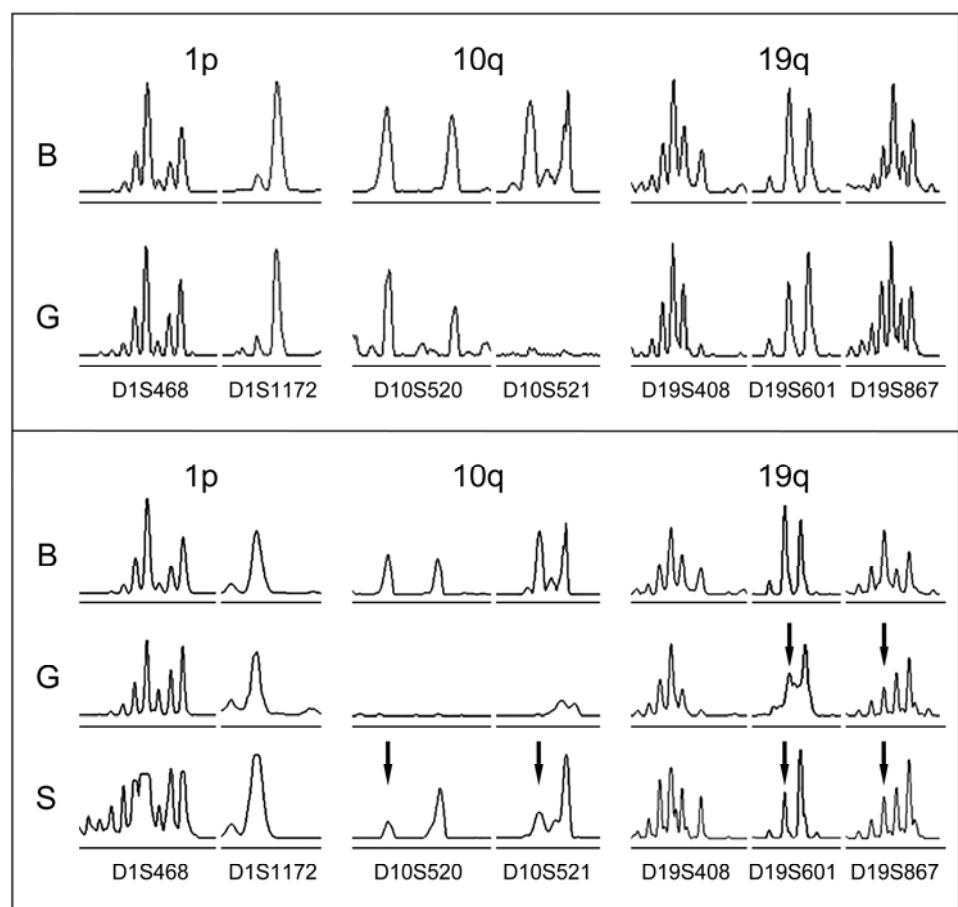
the sarcomatous component.

Fig. 1.

Fig. 2.

Fig. 3.